Supporting Information for (c8ta11072g)

An Fe-doped nickel selenide nanorod/nanosheet hierarchical array for efficient overall water splitting

Zexian Zou,‡ Xiangyu Wang,‡ Jiansong Huang, Zhengcui Wu* and Feng Gao*

Anhui Laboratory of Molecule-Based Materials (State Key Laboratory Cultivation Base), The Key Laboratory of Functional Molecular Solids, Ministry of Education, College of Chemistry and Materials Science, Anhui Normal University, Wuhu 241002, P. R. China.

‡ These authors contributed equally to this work.

*Corresponding author. E-mail: zhengcui@mail.ahnu.edu.cn; fgao@mail.ahnu.edu.cn.

Tel.: +86 553 3869302; Fax: +86 553 3869302.

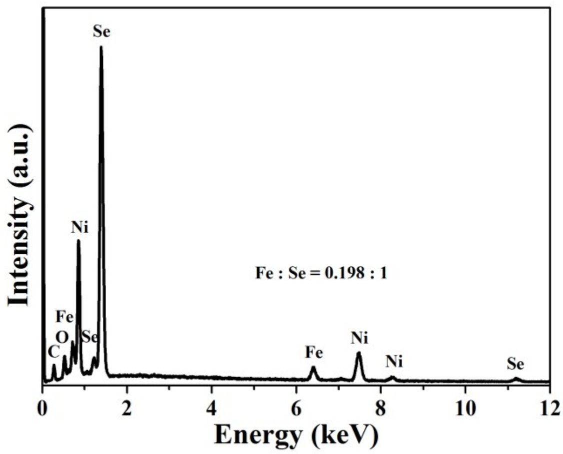

Fig. S1 The EDX result of $Fe_{7.4\%}$-NiSe.

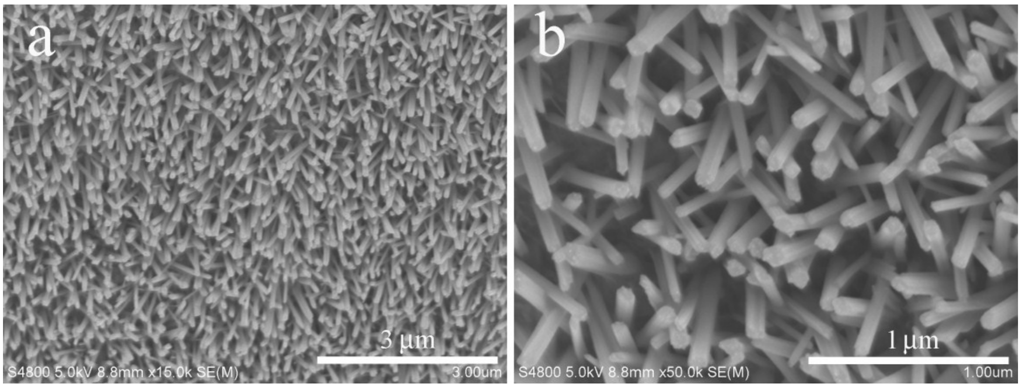

Fig. S2 The SEM images of NiSe nanorods array.

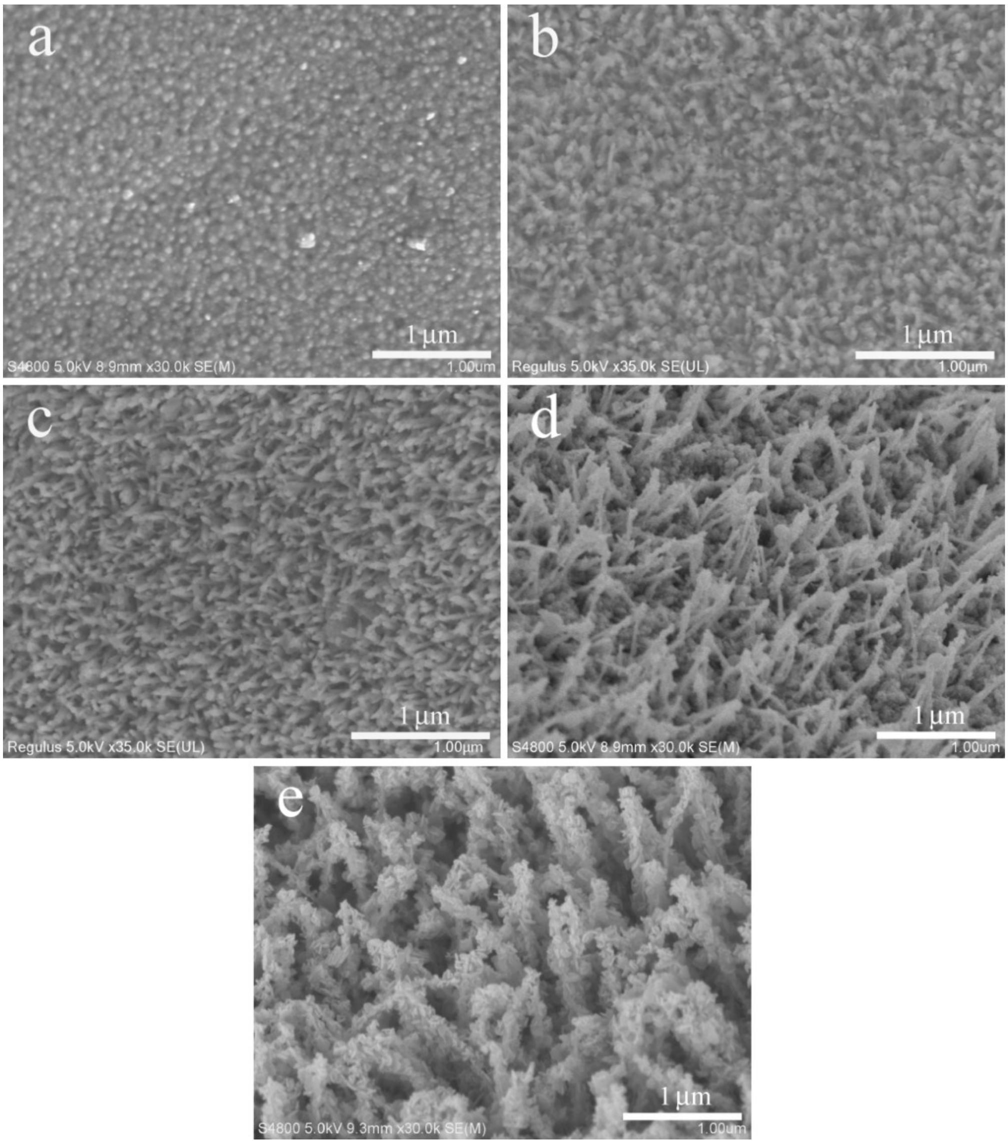

Fig. S3 Time resolved experiments of $Fe_{7.4\%}$-NiSe nanorod/nanosheet hierarchical array. (a) 0.5 h. (b) 1 h. (c) 2 h. (d) 3 h. (e) 8h.

Table S1 The comparison of OER activity of $Fe_{7.4\%}$-NiSe with some representative Ni-based selenide catalysts.

Catalyst	Electrolyte	Loading ($mg\ cm^{-2}$)	η(mV) @j ($mA\ cm^{-2}$)	Tafel Slope ($mV\ dec^{-1}$)	Electrode	Reference
Fe-doped $NiSe/Ni_3Se_2$ nanorods	1 M KOH	3.0	290@60	61	Ni foam	1
Porous $(Ni_{0.75}Fe_{0.25})Se_2$ nanosheets	1 M KOH	~1.5	255@35	47.2	Carbon fiber cloth	2
Rose-like $Ni_{0.76}Fe_{0.24}Se$	1 M KOH	6.6	197@10, 294@200	56	Ni foam	3
NiSe@NiOOH	1 M KOH	-	332@50	162	Ni foam	4
Urchin-like $Ni_{1.12}Fe_{0.49}Se_2$	1 M KOH	0.45	227@10	37.9	Glassy Carbon	5
Ni_3Se_2	0.1 M KOH	0.2	470@1.32	46	Glassy Carbon	6
NiSe nanowire	1 M KOH	-	400@35	54	Ni foam	7
Ni_3Se_2 film	0.3 M KOH	-	~ 270@10	142.8	Ni foam	8
Ni_3Se_2 nanoforest	1 M KOH	8.87	242@20, 353@100	144	Ni foam	9
NiSe nanowire film	1 M KOH	2.8	270@20	64	Ni foam	10
$NiSe–NiO_x$	1 M KOH	4.25	243@10	128	Ni foam	11
Co-doped nickel selenide/C	1 M KOH	-	275@30, 300@50	63	Ni foam	12
$Fe_{7.4\%}$-NiSe	1 M KOH	3.1	231@50, 254@200	43.0	Ni foam	This work

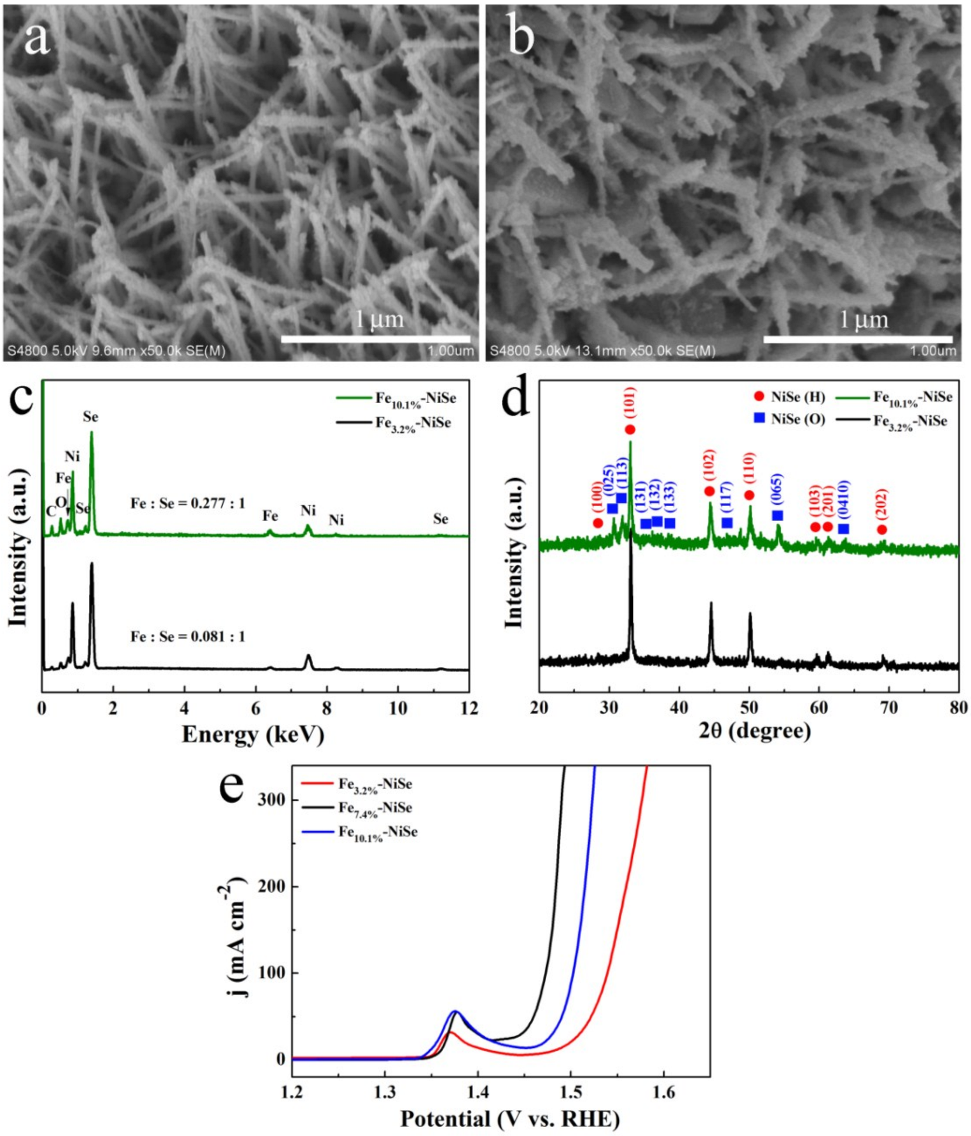

Fig. S4 (a, b) The SEM images of the Fe-doped NiSe products with Fe content of 3.2% and 10.1%, respectively. (c, d) The EDX spectra and the XRD patterns of the Fe-doped NiSe products with Fe content of 3.2% and 10.1%, respectively. (e) The OER polarization curves of the Fe-doped NiSe products with different Fe content.

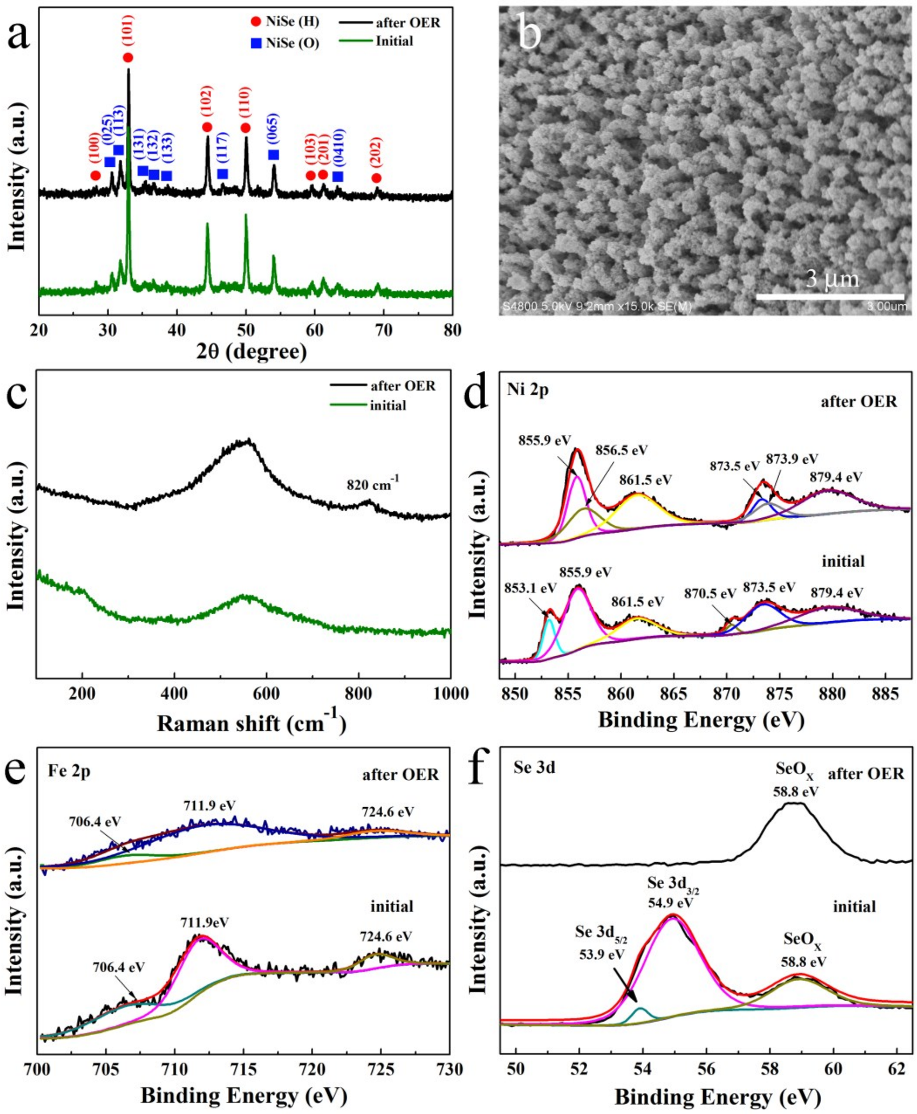

Fig. S5 The XRD pattern (a), the SEM image (b), the Raman spectrum (c), the XPS spectra of Ni 2p (d), Fe 2p (e), and Se 3d (f) of $Fe_{7.4\%}$-NiSe after 22 h OER chronopotentiometry test at an overpotential of 217 mV.

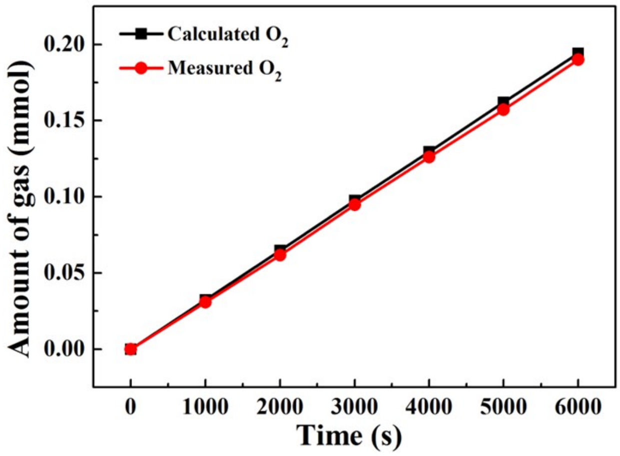

Fig. S6 The electrocatalytic efficiency of $Fe_{7.4\%}$-NiSe for OER at 50 mA cm^{-2}.

Table S2 The comparison of HER activity of $Fe_{7.4\%}$-NiSe with some representative Ni-based selenide catalysts.

Catalyst	Electrolyte	Loading (mg cm^{-2})	η (mV) @j(mA cm^{-2})	Tafel Slope (mV dec^{-1})	Electrode	Reference
Fe-doped $NiSe/Ni_3Se_2$ nanorods	1 M KOH	3.0	140@10	-	Ni foam	[1]
Ni_3Se_2 nanoforest	1 M KOH	8.87	203@10, 279@100	79	Ni foam	[9]
NiSe Nanowire film	1 M KOH	2.8	96@10	120	Ni foam	[10]
$CoNi_2Se_4$ nanoflake film	1 M KOH	4.7	220@10	-	Carbon fiber Paper	[13]
Porous $NiSe_2$ nanosheets	1 M KOH	~ 0.46	184@10	76.6	Ni foam	[14]
$NiSe_2$ nanocrystals	1 M KOH	1	540@10	139	Rotating disk electrode	[15]
Cactuslike Ni_3Se_4	1 M KOH	2.45	206@50	156	Ni foam	[16]
$MoSe_2$−NiSe	0.5 M H_2SO_4	~ 0.285	210@10	56	glassy carbon electrode	[17]
$Fe_{7.4\%}$-NiSe	1 M KOH	3.1	163@10, 265@100	71.4	Ni foam	This work

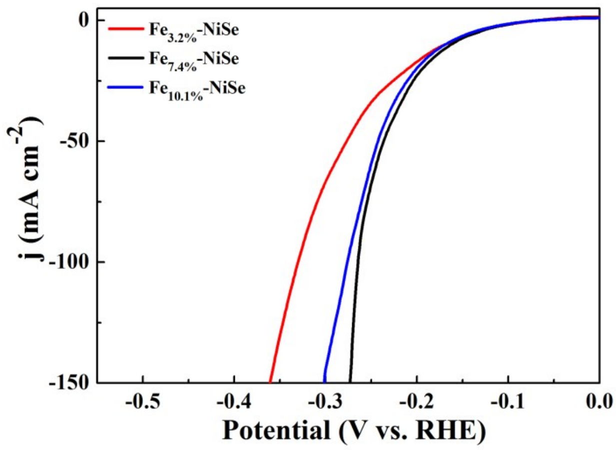

Fig. S7 The HER polarization curves of the Fe-doped NiSe products with different Fe content.

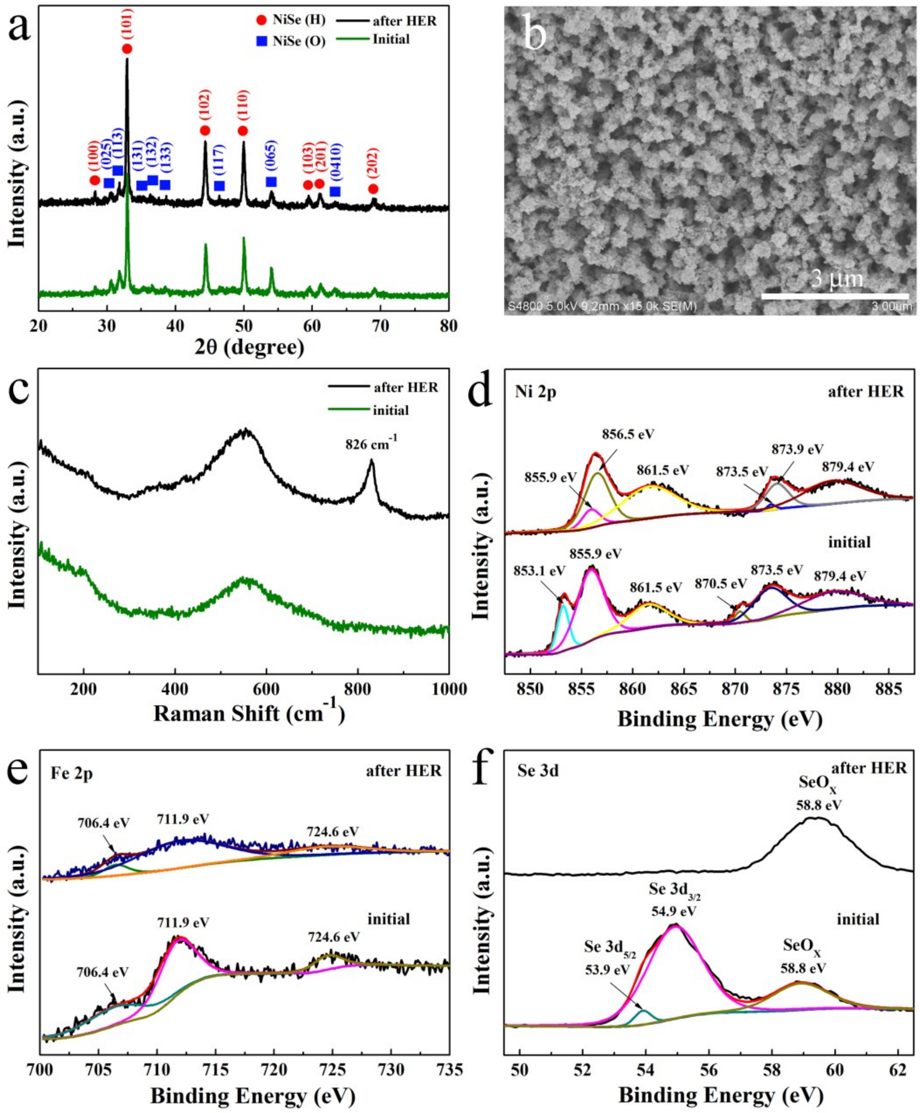

Fig. S8 The XRD pattern (a), the SEM image (b), the Raman spectrum (c), the XPS spectra of Ni 2p (d), Fe 2p (e) and Se 3d (f) of $Fe_{7.4\%}$-NiSe after 22 h HER chronopotentiometry test at an overpotential of 195 mV.

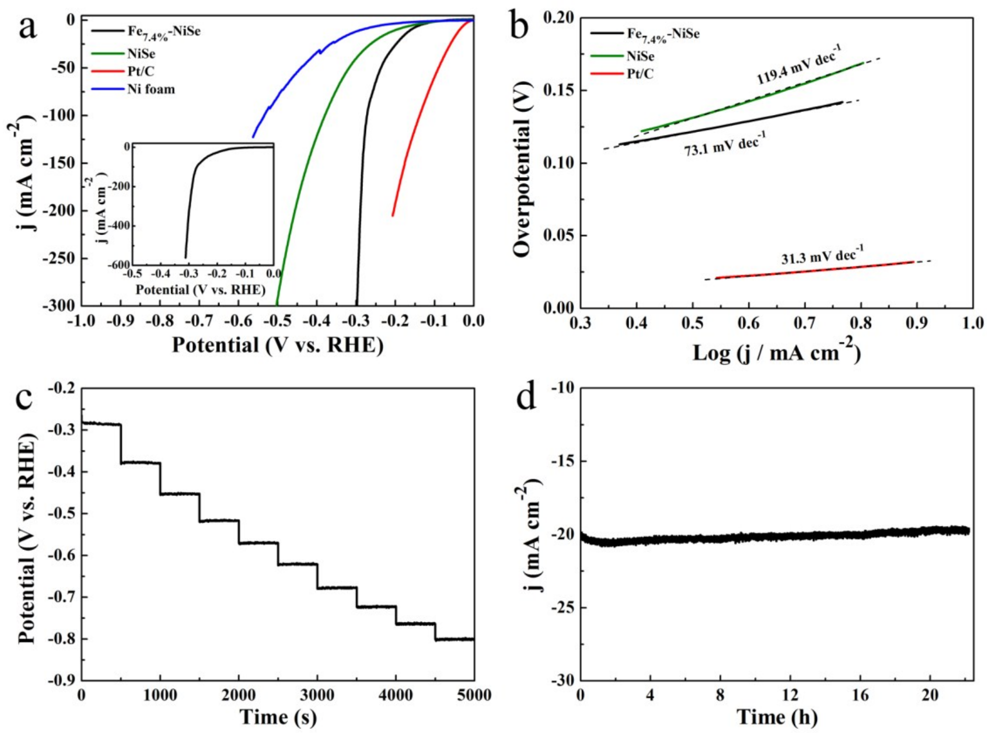

Fig. S9 The HER performances of the catalysts with a carbon rod as the counter electrode. (a) The HER polarization curves of $Fe_{7.4\%}$-NiSe, NiSe, Pt/C, and Ni foam. (b) The corresponding Tafel plots of $Fe_{7.4\%}$-NiSe, NiSe, and Pt/C. (c) The multi-step chronopotentiometric curve of $Fe_{7.4\%}$-NiSe without iR-compensation. (d) The chronoamperometric curve of $Fe_{7.4\%}$-NiSe for 22 h.

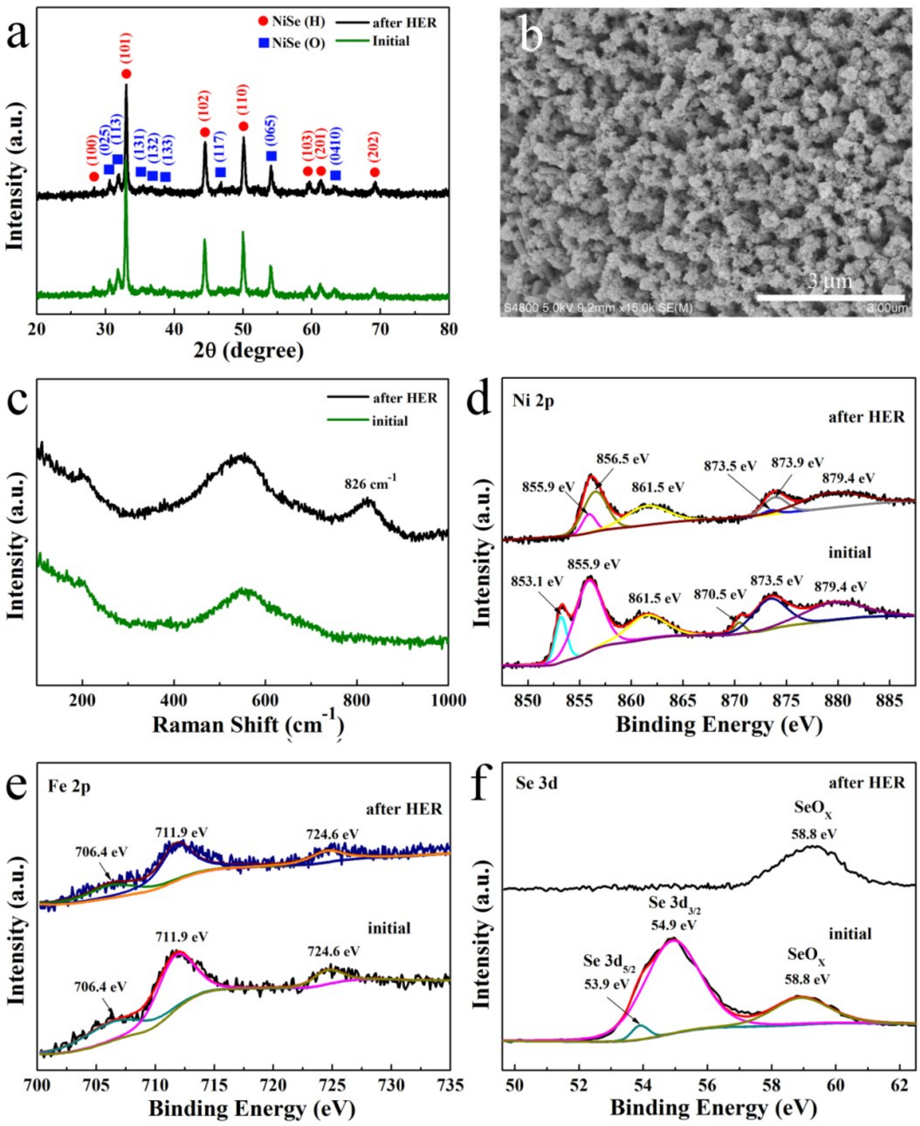

Fig. S10 The XRD pattern (a), the SEM image (b), the Raman spectrum (c), the XPS spectra of Ni 2p (d), Fe 2p (e) and Se 3d (f) of $Fe_{7.4\%}$-NiSe after 22 h HER chronopotentiometry test with a carbon rod as the counter electrode.

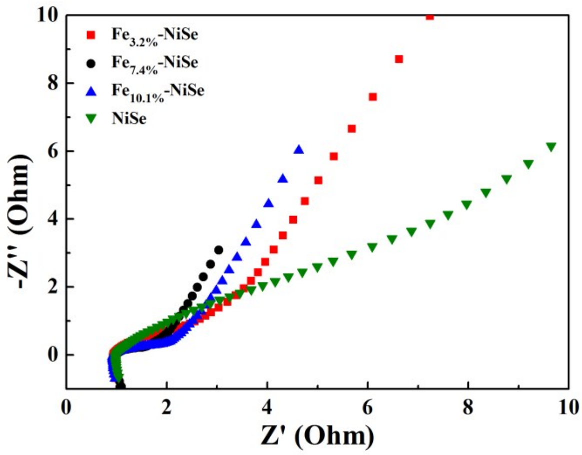

Fig. S11 The Nyquist diagrams of the Fe-doped NiSe with different Fe content and undoped NiSe.

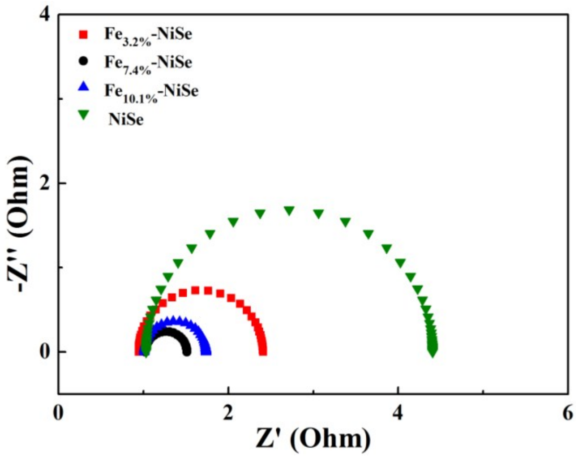

Fig. S12 The fitting results of the semicircles of EIS of the Fe-doped NiSe with different Fe content and undoped NiSe.

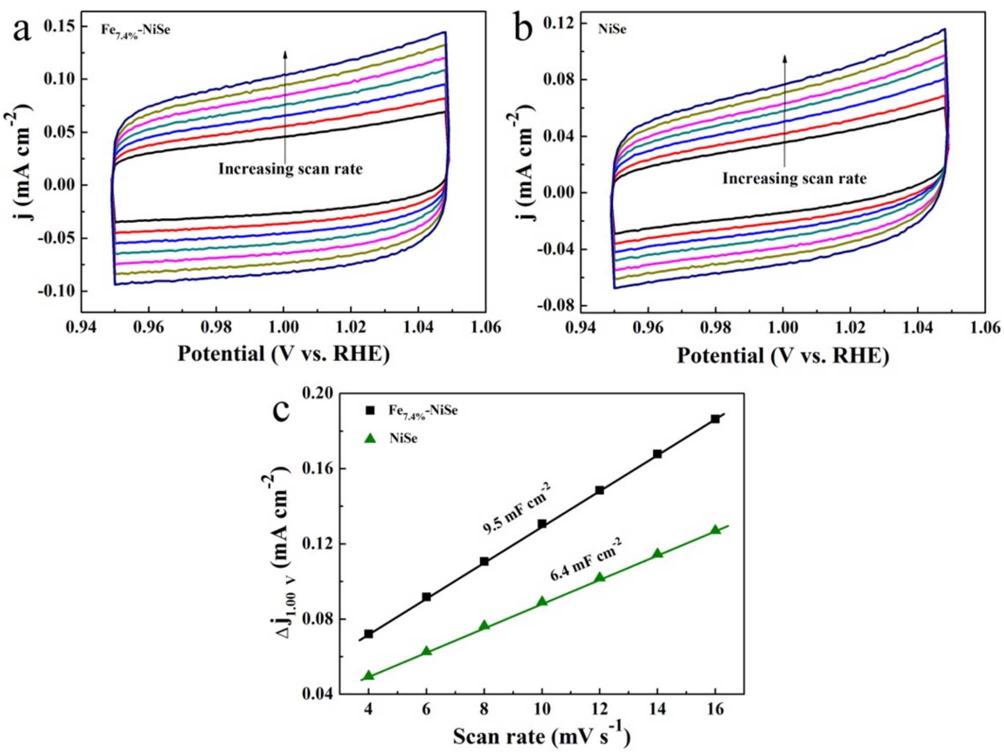

Fig. S13 The cyclic voltammograms of $Fe_{7.4\%}$-NiSe (a) and NiSe (b) at different sweep rates of 4, 6, 8, 10, 12, 14, and 16 mV s^{-1}. (d) The capacitive currents at 1.00 V versus RHE with different sweep rates.

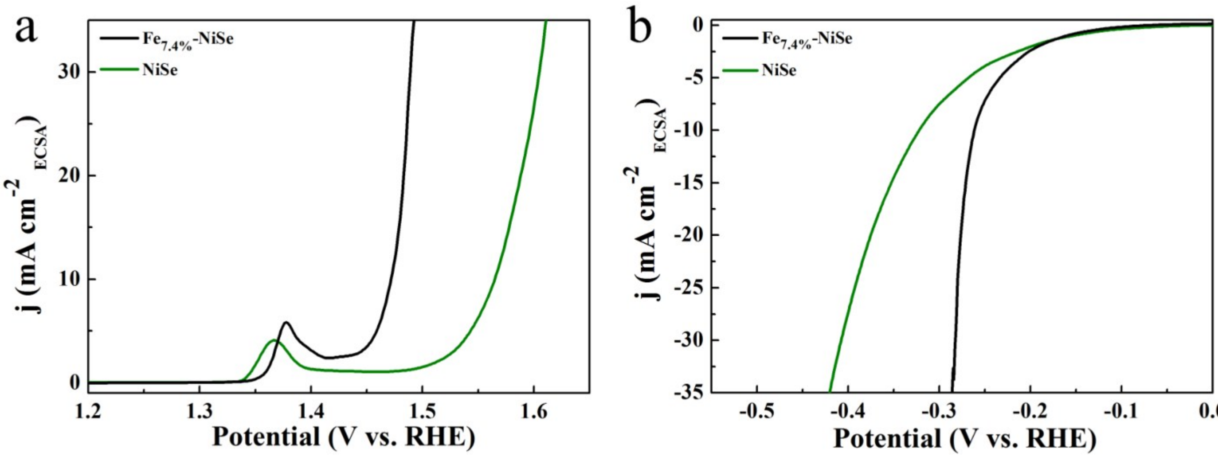

Fig. S14 The ECSA-normalized LSV curves of $Fe_{7.4\%}$-NiSe and NiSe for OER (a) and HER (b) with Pt wire as the counter electrode.

Table S3 Comparison of overall water-splitting performance of $Fe_{7.4\%}$-NiSe with some representative Ni-based selenide catalysts.

Catalyst	Electrolyte	Potential (V) @j(mA cm^{-2})	Electrode	Reference
Fe-doped NiSe/Ni_3Se_2 nanorods	1 M KOH	1.64@10	Ni foam	1
Ni_3Se_2 nanoforest	1 M KOH	1.612@10	Ni foam	9
NiSe nanowire film	1 M KOH	1.63@10	Ni foam	10
Co-doped nickel selenide/C	1 M KOH	1.6@10	Ni foam	12
$CoNi_2Se_4$ nanoflake film	1 M KOH	1.61@10	Carbon fiber Paper	13
Co-doped $NiSe_2$ nanoparticles	1 M KOH	1.62@10	Ti plate	18
Ni_3Se_2 film	1 M KOH	1.65@10	Cu foam	19
$Fe_{7.4\%}$-NiSe	1 M KOH	1.585@10	Ni foam	This work

References

1 J. Du, A. Yu, Z. Zou and C. Xu, *Inorg. Chem. Front.*, 2018, **5**, 814−818.

2 Z. Wang, J. Li, X. Tian, X. Wang, Y. Yu, K. A. Owusu, L. He and L. Mai, *ACS Appl. Mater. Interfaces*, 2016, **8**, 19386−19392.

3 J. Yu, G. Cheng and W. Luo, *Nano Res.*, 2018, **11**, 2149−2158.

4 X. Li, G. Q. Han, Y. R. Liu, B. Dong, W. H. Hu, X. Shang, Y. M. Chai and C. G. Liu, *ACS Appl. Mater. Interfaces*, 2016, **8**, 20057−20066.

5 Y. Du, G. Cheng and W. Luo, *Nanoscale*, 2017, **9**, 6821−6825.

6 K. Xu, H. Ding, H. Lv, S. Tao, P. Chen, X. Wu, W. Chu, C. Wu and Y. Xie, *ACS Catal.*, 2016, **7**, 310−315.

7 K. Xu, H. Ding, K. Jia, X. Lu, P. Chen, T. Zhou, H. Cheng, S. Liu, C. Wu and Y. Xie, *Angew. Chem. Int. Ed.*, 2016, **55**, 1710−1713.

8 A. T. Swesi, J. Masud and M. Nath, *Energy Environ. Sci.*, 2016, **9**, 1771−1782.

9 R. Xu, R. Wu, Y. Shi, J. Zhang and B. Zhang, *Nano Energy*, 2016, **24**, 103−110.

10 C. Tang, N. Cheng, Z. Pu, W. Xing and X. Sun, *Angew. Chem. Int. Ed.*, 2015, **54**, 9351−9355.

11 R. Gao, G.-D. Li, J. Hu, Y. Wu, X. Lian, D. Wang and X. Zou, *Catal. Sci. Technol.*, 2016, **6**, 8268−8275.

12 F. Ming, H. Liang, H. Shi, X. Xu, G. Mei and Z. Wang, *J. Mater. Chem. A*, 2016, **4**, 15148−15155.

13 B. G. Amin, A. T. Swesi, J. Masud and M. Nath, *Chem. Commun.*, 2017, **53**, 5412−5415.

14 H. Liang, L. Li, F. Meng, L. Dang, J. Zhuo, A. Forticaux, Z. Wang and S. Jin, *Chem. Mater.*, 2015, **27**, 5702−5711.

15 I. H. Kwak, H. S. Im, D. M. Jang, Y. W. Kim, K. Park, Y. R. Lim, E. H. Cha and J. Park, *ACS Appl. Mater. Interfaces*, 2016, **8**, 5327−5334.

16 S. Anantharaj, J. Kennedy and S. Kundu, *ACS Appl. Mater. Interfaces*, 2017, **9**, 8714−8728.

17 X. Zhou, Y. Liu, H. Ju, B. Pan, J. Zhu, T. Ding, C. Wang and Q. Yang, *Chem. Mater.*, 2016, **28**, 1838−1846.

18 T. Liu, A. M. Asiri and X. Sun, *Nanoscale*, 2016, **8**, 3911−3915.

19 J. Shi, J. Hu, Y. Luo, X. Sun and A. M. Asiri, *Catal. Sci. Technol.*, 2015, **5**, 4954−4958.